

PAPER • OPEN ACCESS

## Development of EPID-based dosimetry for FFF-beam verification in radiation therapy

To cite this article: S Thongsawad *et al* 2019 *J. Phys.: Conf. Ser.* **1285** 012031

View the [article online](#) for updates and enhancements.



**IOP | ebooks™**

Bringing you innovative digital publishing with leading voices to create your essential collection of books in STEM research.

Start exploring the collection - download the first chapter of every title for free.

# Development of EPID-based dosimetry for FFF-beam verification in radiation therapy

S Thongsawad<sup>1</sup>, T Chanton<sup>2</sup>, N Saiyo<sup>1</sup> and N Udee<sup>2</sup>

<sup>1</sup>Department of Radiation Oncology, Chulabhorn Royal Academy, Bangkok, Thailand

<sup>2</sup>Department of Radiological Technology, Faculty of Allied Health Sciences, Naresuan University, Mueang, Phitsanulok, Thailand.

E-mail: sangutid.tho@pccms.ac.th

**Abstract.** The purpose of this study was to develop Electronic Portal Imaging Devices (EPID)-based dosimetry for Flattening-Filter-Free (FFF) beam verification. All radiation measurements were performed with source to imager distances (SID) of 150 cm to reduce saturation effect. EPID images were converted to radiation absorbed dose with our algorithm including four parameters: linearity of dose response with Monitor Unit (MU), beam profile correction, collimator scatter, and scatter kernel. The Calibration Units (CU) of image were scaled to dose (Gy) by using linearity of dose response with MU. Off-axis response differences between EPID and water were reduced with beam profile correction. Scatter kernel was applied to EPID images to reduce the residual error. The algorithm accuracy was validated with 12 arcs of Volumetric Modulated Arc Therapy (VMAT) plans by using gamma analysis comparing between EPID-based dosimetry and a plane dose distribution of Treatment Planning Systems (TPS). Gamma Passing Rates (GPR) were used to determine the dose agreements with criteria of 2%, 2 mm and 3%, 3 mm. The mean of GPR was 97.91%, and 99.62% for criteria of 2%, 2 mm and 3%, 3 mm, respectively. Our EPID-based dosimetry showed good agreement with plane dose distribution in water. These results indicated that our EPID-based dosimetry can perform FFF-beam verification.

## 1. Introduction

Patient-specific quality assurance (QA) is a process to verify the radiation dose agreement between a beam delivery and calculation using a treatment planning systems (TPS) [1, 2]. Many devices have been developed for patient-specific QA with different characteristics such as ionization chamber arrays, diode arrays, film dosimetry, and gel dosimetry. Electronic portal imaging devices (EPIDs) are the radiation imager detector attached to the linear accelerators (LINACs) which are used for patient position verification [3]. With the benefit of spatial resolution, immediate signal readout, and sensitivity, EPIDs have been developed to perform a radiation dose measurement in patient-specific QA process with different methods [4-6]. However, the reading saturation effect can be occurred when a measurement was performed with high dose rate in flattening-filter-free (FFF) beams [7-10]. FFF beams were developed to increase a dose rate by removing flattening filter in a head of LINACs machine, which were used for the advance radiation technique (Stereotactic Radiation Surgery: SRS and Stereotactic Body Radiotherapy: SBRT) to reduce treatment time [11-13]. Many studies presented the method to reduce saturation effect such as placing a plastic on EPID surface, increasing source-to-imager distance (SID). For flattening filter (FF) beam verification, the regular SID of 100 to 105 cm



was used to perform patient-specific QA. Tyner et al. [14] found 1 cm of water-equivalent plastic placed on EPID surface can reduce saturation effect for dose rate less than 1,000 Monitor Unit (MU)/min. Nicoli et al. [15] found the suitable distance could be more than 150 cm to reduce saturation effect for FFF beams. Chuter et al. [16] found SID of 160 cm can be used to remove saturation effect for dose rate less than 800 MU/min. Several studies have developed EPID-based dosimetry for FFF-beam verification with various methods. Miri et al. [7] developed a method to convert EPID images to 2D dose in virtual phantom with two steps as follows: (1) incident fluence modeling, and (2) fluence to dose in water phantom modeling. Podesta et al. [9] developed EPID-based dosimetry model for FFF beams with time-resolved assessment. Wendling et al. [17] developed a back-projection EPID dosimetry method to reconstruct the dose within the patient or phantom using a dose-response matrix, scatter corrections, inverse square law factor, and transmission factor of the phantom. This study, we emphasized on the simple method to develop EPID-based dosimetry for FFF-beam verification. EPID images were converted to absorbed dose in water at depth of 10 cm including four parameters: linearity of dose response with MU, beam profile correction, collimator scatter, and scatter kernel. In addition, the extended SID was applied during measurement to reduce signal saturation.

## 2. Materials and methods

TrueBeam LINACs (Varian Medical Systems, Palo Alto, CA) equipped with amorphous silicon (a-Si) 1000 EPID was used to acquire images for patient-specific QA. The radiation was delivered with 6 X-FFF energy and integrated mode. Dose calculation was performed using Eclipse TPS version 13.6 (Varian Medical Systems, Palo Alto, CA).

### 2.1 EPID-based dosimetry model

The standard image calibration was performed prior use following the manufacturer's recommendations [27] including dark field, flood field, and dose normalization. In this study, the extended SID of 150 cm was used to reduce saturation effect, and a simple model was used for EPID-base dosimetry. EPID images ( $EPID_{x,y}$ ) were converted to absorbed dose in water at depth of 10 cm ( $D$ ) as follows:

$$D = (EPID_{x,y} \times M_{FFF}^{2D} \times S_{fs} \times f_{dose}) \otimes^{-1} K_{water} \quad (1)$$

First step, the calibration units (CU) of EPID image were scaled to dose by using linearity function ( $f_{dose}$ ) between CU and absorbed dose in water at depth 10 cm. Linearity function ( $f_{dose}$ ) can be written as follows:

$$y = Ax + B \quad (2)$$

where  $y$  is linearity function ( $f_{dose}$ ),  $A$  is the first constant parameter for linearity function,  $x$  is CU of EPID image, and  $B$  is the second constant parameter for linearity function.

Second step, beam profile difference between EPID and water was corrected with ratio between diagonal profile of water and profile of EPID which was named beam profile correction ( $M_{FFF}^{2D}$ ). Polynomial fourth order function was used for beam profile correction factor to improve accuracy of curve fitting. It can be written as follows:

$$y = Cx^4 + Dx^3 + Ex^2 + Fx + G \quad (3)$$

where  $y$  is beam profile correction factor ( $M_{FFF}^{2D}$ ),  $x$  is distance from beam central-axis,  $C$ ,  $D$ ,  $E$ ,  $F$ ,  $G$  is the first, second, third, fourth, and fifth constant parameter, respectively.

Third step, the collimator scatter difference between EPID and water was corrected with response ratio between EPID collimator scatter and water collimator scatter which was named collimator scatter correction ( $S_{fs}$ ). Polynomial third order function was used for collimator scatter correction ( $S_{fs}$ ) to improve accuracy of curve fitting. It can be written as follows:

$$y = Hx^3 + Ix^2 + Jx + K \quad (4)$$

where  $y$  is collimator scatter correction ( $S_{fs}$ ),  $x$  is the equivalent square radiation field size,  $H$ ,  $I$ ,  $J$ ,  $K$  is the first, second, third, fourth, and fifth constant parameter, respectively.

The fourth step, residual error between three previous steps and water distribution was corrected with water kernel ( $K_{water}$ ) using King et al. [18] method. Exponential function was used for water kernel ( $K_{water}$ ) to reduce residual error. It can be written as follows:

$$y = e^{-(a_1r)} + a_2e^{-(a_3r)} + a_4e^{-(a_5r)} \quad (5)$$

where  $y$  is water kernel ( $K_{water}$ ),  $r$  is the distance from beam central-axis,  $a_1$ ,  $a_2$ ,  $a_3$ ,  $a_4$ ,  $a_5$  is the first, second, third, fourth, and fifth constant parameter, respectively.

## 2.2 Model validation

The model accuracy was validated with 12 arcs of VMAT plans in brain case by comparing between our EPID-based dosimetry and TPS dose calculation in water. In addition, MapCHECK diode arrays (Sun Nuclear Corporation, Melbourne, FL) were used to confirm the result of model validation by comparing between diode array measurements and TPS dose calculation in water. Figure 1 shows flowchart of model validation. Plan data were transferred to water phantom and then dose was calculated using TPS algorithms. The plane dose at depth of 10 cm were exported as DICOM format to compare with EPID-based dosimetry. Gamma passing rates (GPR) were used to determine the agreement between EPID-based dosimetry and TPS dose calculation using criteria of 3%, 3mm, 2%, 2mm, and cut-off threshold at 10%.

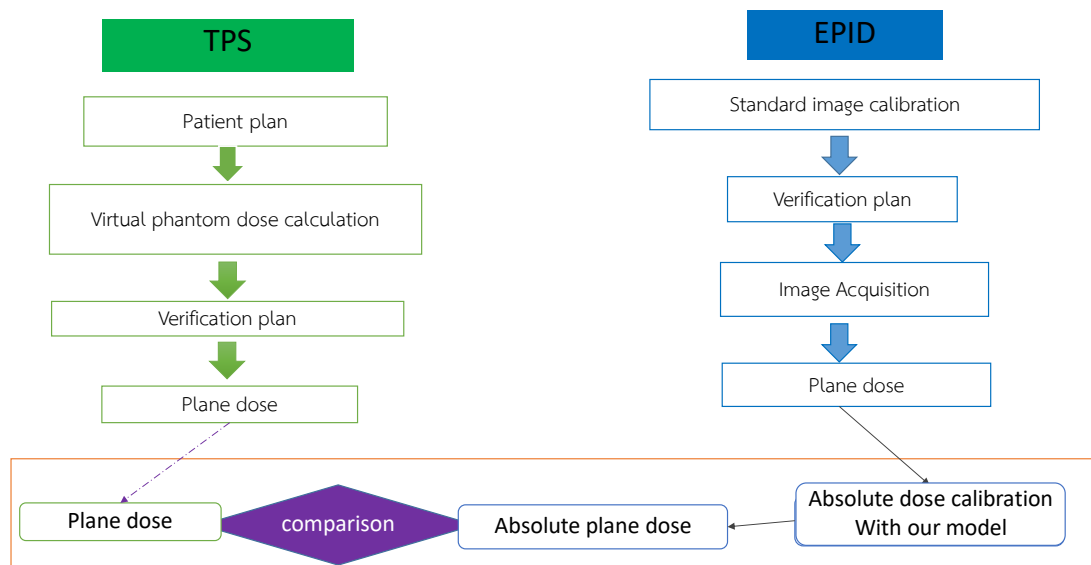


**Figure 1.** Flowchart of model validation.

## 3. Results

### 3.1 EPID-based dosimetry model

Linearity function ( $f_{dose}$ ) between CU and absorbed dose was  $y = 0.008x + 0.011$  for 6X-FFF. Figure 2 shows the linearity curve between CU and absorbed dose at depth of 10 cm.

Polynomial function of beam profile correction ( $M_{FFF}^{2D}$ ) was  $y = 3.9 \times 10^{-4}x^4 + 1.7 \times 10^{-2}x^3 - 0.29x^2 + 0.42x + 100$ . Figure 3 demonstrates a beam profile correction curve for 6X-FFF.

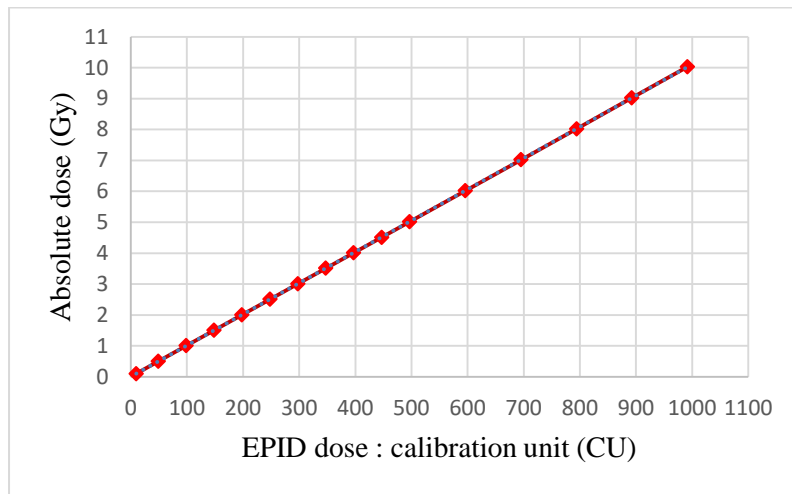


**Figure 2.** Linear calibration curve for 6X-FFF.

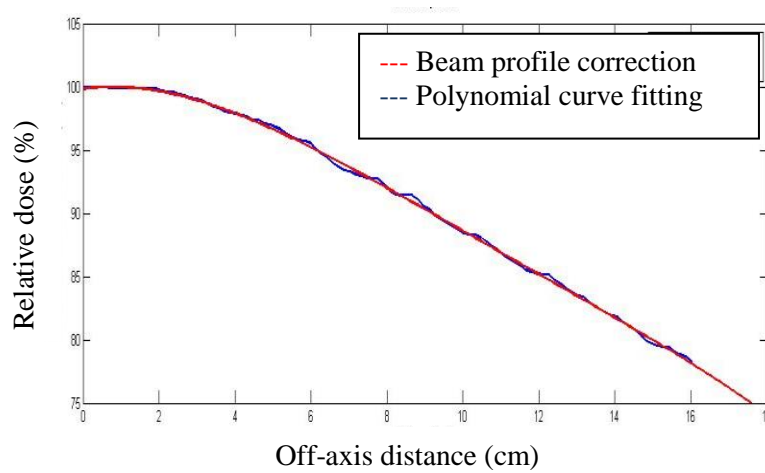


**Figure 3.** Beam profile correction curve for 6X-FFF.

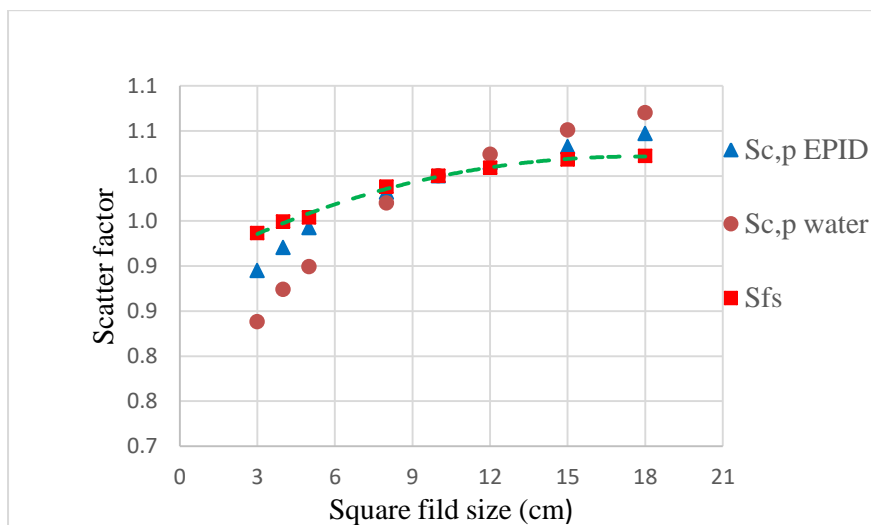


**Figure 4.** Collimator scatter correction ( $S_{fs}$ ), EPID collimator scatter response ( $S_{c,p}$  EPID), and water collimator scatter response ( $S_{c,p}$  water) for 6X-FFF.

Polynomial function of collimator scatter correction ( $S_{fs}$ ) was  $4 \times 10^{-6}x^3 - 5 \times 10^{-3}x^2 + 0.02x + 0.89$  for 6X. Figure 4 demonstrates collimator scatter correction ( $S_{fs}$ ), EPID collimator scatter response ( $S_{c,p}$  EPID), and water collimator scatter response ( $S_{c,p}$  water) for 6X-FFF.

Water kernel function ( $K_{water}$ ) was  $e^{(-25*r)} + (8 \times 10^{-4})e^{(-1.5*r)} + (1.7 \times 10^{-5})e^{(-0.22*r)}$ , where r is distance from centre. Figure 5 shows water kernel ( $K_{water}$ ) for 6X-FFF.

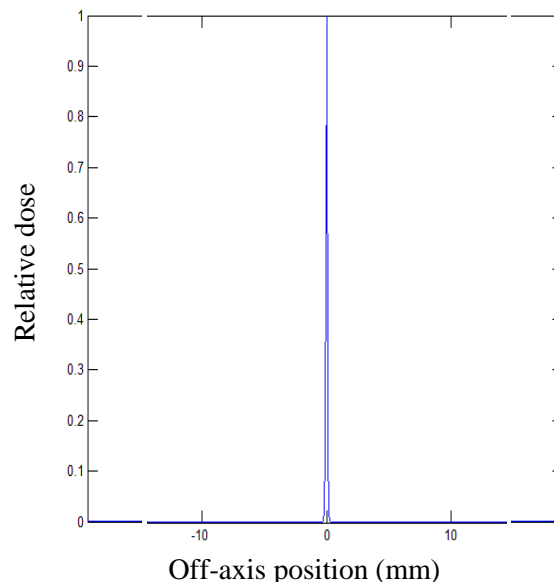


**Figure 5.** Water kernel ( $K_{water}$ ) for 6X-FFF.

**Table 1.** Results of GPR for model validation by comparing between our EPID-based dosimetry and TPS dose calculation in water.

Plans	GPR	
	3%,3mm	2%,2mm
<u>Plan 1</u>		
Arc no.1	99.1	96.15
Arc no.2	99.9	99.40
Arc no.3	100	99.98
Arc no.4	100	99.66
Arc no.5	100	99.76
<u>Plan 2</u>		
Arc no.1	100	99.91
Arc no.2	100	99.95
Arc no.3	98.6	94.74
Arc no.4	99.1	94.3
<u>Plan 3</u>		
Arc no.1	98.9	93.6
Arc no.2	99.8	97.5
Arc no.3	100	99.92
<u>Mean (SD)</u>	99.62 (0.53)	97.91 (2.52)

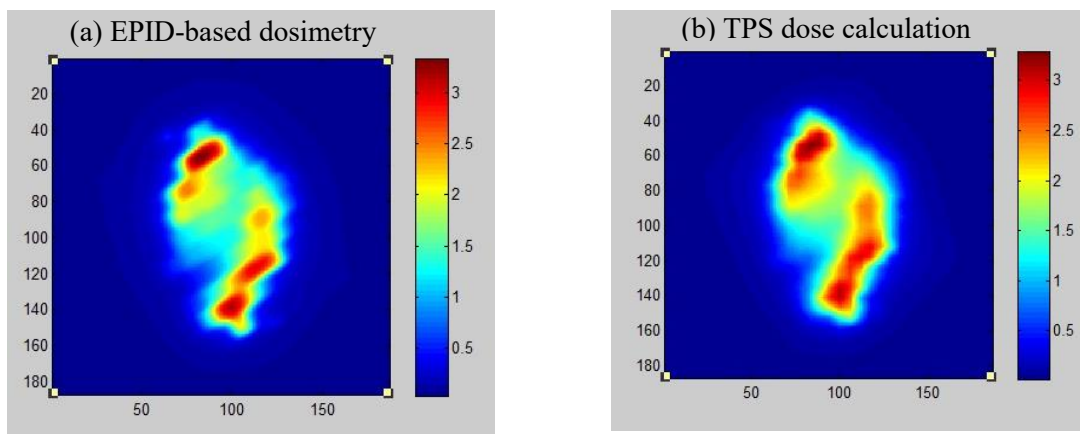
**Table 2.** Results of comparison between MapCHECK measurements and TPS dose calculation in water.

Plans	GPR	
	3%,3mm	2%,2mm
<u>Plan 1</u>		
Arc no.1	97.1	96.9
Arc no.2	100	100
Arc no.3	100	100
Arc no.4	100	100
Arc no.5	100	97.1
<u>Plan 2</u>		
Arc no.1	100	98.6
Arc no.2	98.6	97
Arc no.3	98.5	95.6
Arc no.4	100	100
<u>Plan 3</u>		
Arc no.1	96	91.3
Arc no.2	100	95.6
Arc no.3	100	100
<u>Mean (SD)</u>	99.18 (1.37)	97.68 (2.67)

### 3.2 Model validation

Table 1 shows the results of model validation for 6X-FFF (brain plans) by comparing between our EPID-based dosimetry and TPS dose calculation in water. For gamma criteria of 3%, 3mm, mean of GPR was 99.62%, the lowest GPR was 98.6%, and the highest GPR was 100%. For gamma criteria of 2%, 2mm, mean of GPR was 97.91%, the lowest GPR was 93.6%, and the highest GPR was 99.98%.

Table 2 shows results of comparison between MapCHECK measurements and TPS dose calculation in water. For gamma criteria of 3%, 3mm, mean of GPR was 99.18%, the lowest GPR was 96.0%, and the highest GPR was 100%. For gamma criteria of 2%, 2mm, mean of GPR was 97.68%, the lowest GPR was 95.6%, and the highest GPR was 100%. Figure 6 shows an example plane dose comparison between EPID-based dosimetry and TPS dose calculation.

**Figure 6.** Example plane dose comparison between (a) EPID-based dosimetry and (b) TPS dose calculation.

#### 4. Discussions

Our previous study [19] have evaluated EPID signal saturation with SID, and we found signal saturation was not occurred at 150 cm SID for 6 X-FFF; hence, 150 cm was applied during image acquisition in this study.

There are two methods for EPID-based dosimetry. First, photon fluence was predicted to dose distribution at EPID using algorithm from Treatment Planning Systems (TPS) or independent algorithm, which is then compared with EPID measurement [20]. Second, EPID images were converted to absorbed dose at water, and then compared with dose calculation by TPS [21, 22]. The benefit of second method is a potential to directly verify the accuracy of TPS algorithm [17, 23]. Our EPID-based model also performed as a second method by converting images to dose distribution in water at 10 cm depth.

MapCHECK measurement represents a traditional method for patient-specific QA with low spatial resolution detectors (445 diodes) compared to EPIDs with high spatial resolution (1024x768 pixels). The results of patient-specific QA between EPID-based dosimetry (Table 1) and MapCHECK measurements (Table 2) indicated that EPID-based dosimetry has slightly better agreement than MapCHECK that could be the effect of spatial resolution detectors which was described by Benjamin et al. [24]. The result of EPID-based dosimetry compared to MapCHECK was similar to other publication [7].

There are two modes to acquire EPID images for dosimetry: integrated mode, and cine mode. For integrated mode, EPID captures a single image consisting of the average number of frames acquired during radiation delivery [25]. For cine mode, a sequence of multiple images are captured during radiation delivery instead of a single integrated image [5]. Cine mode is suitable for VMAT patient-specific QA with a good potential to assess each control point. Since cine mode is synchronized to beam pulses, the frame acquisition rate depends on dose rate [26]. Our study, images were acquired with integrated mode to reduce dose rate effect from cine mode. Future study, we will focus on cine mode for FFF beams.

#### 5. Conclusion

Our EPID-based dosimetry showed good agreements with plane dose distribution in water. The study indicated that our EPID-based dosimetry with a simple method can perform FFF beam verification for patient-specific QA.

#### References

- [1] Depuydt T, Van Esch A, Huyskens DP. A quantitative evaluation of IMRT dose distributions: refinement and clinical assessment of the gamma evaluation. *Radiother Oncol.* 2002;**62**(3):309-19.
- [2] Agazaryan N, Solberg TD, DeMarco JJ. Patient specific quality assurance for the delivery of intensity modulated radiotherapy. *J Appl Clin Med Phys.* 2003;**4**(1):40-50.
- [3] Van Elmpt W, McDermott L, Nijsten S, Wendling M, Lambin P, Mijnheer B. A literature review of electronic portal imaging for radiotherapy dosimeter. *Radiother Oncol.* 2008;**88**:289-309.
- [4] Van Esch A, Depuydt T, Huyskens DP. The use of an aSi-based EPID for routine absolute dosimetric pre-treatment verification of dynamic IMRT fields. *Radiother Oncol.* 2004;**71**(2):223-34.
- [5] McCurdy BM, Greer PB. Dosimetric properties of an amorphous-silicon EPID used in continuous acquisition mode for application to dynamic and arc IMRT. *Med Phys.* 2009;**36**(7):3028-39.
- [6] Kirby MC, Glendinning AG. Developments in electronic portal imaging systems. *Br J Radiol.* 2006;**79**(special\_issue\_1):S50-S65.
- [7] Miri N, Keller P, Zwan BJ, Greer P. EPID-based dosimetry to verify IMRT planar dose distribution for the aS1200 EPID and FFF beams. *J Appl Clin Med Phys.* 2016;**17**(6):292-



- 304.
- [8] Pardo E, Novais JC, Molina López MY, Maqueda SR. On flattening filter-free portal dosimetry. *J Appl Clin Med Phys*. 2016;**17**(4):132-45.
  - [9] Podesta M, Nijsten S, Persoon L, Scheib S, Baltes C, Verhaegen F. Time dependent pre-treatment EPID dosimetry for standard and FFF VMAT. *Phys Med Biol*. 2014;**59**(16):4749-68.
  - [10] Xu Z, Kim J, Han J, Hsia AT, Ryu S. Dose rate response of Digital Megavolt Imager detector for flattening filter-free beams. *J Appl Clin Med Phys*. 2018;**19**(4):141-7.
  - [11] Prendergast BM, Popple RA, Clark GM, Spencer SA, Guthrie B, Markert J, et al. Improved clinical efficiency in CNS stereotactic radiosurgery using a flattening filter free linear accelerator. *J Radiosurg SBRT*. 2011;**1**(2):117-22.
  - [12] Xiao Y, Kry SF, Popple R, Yorke E, Papanikolaou N, Stathakis S, et al. Flattening filter-free accelerators: a report from the AAPM Therapy Emerging Technology Assessment Work Group. *J Appl Clin Med Phys*. 2015;**16**(3):12-29.
  - [13] Lai Y, Chen S, Xu C, Shi L, Fu L, Ha H, et al. Dosimetric superiority of flattening filter free beams for single-fraction stereotactic radiosurgery in single brain metastasis. *Oncotarget*. 2016;**8**(21):35272-9.
  - [14] Tyner E, McClean B, McCavana P, af Wetterstedt S. Experimental investigation of the response of an a-Si EPID to an unflattened photon beam from an Elekta Precise linear accelerator. *Med Phys*. 2009;**36**(4):1318-29.
  - [15] Nicolini G, Clivio A, Vanetti E, Krauss H, Fenoglietto P, Cozzi L, et al. Evaluation of an aSi-EPID with flattening filter free beams: applicability to the GLAaS algorithm for portal dosimetry and first experience for pretreatment QA of RapidArc. *Med Physics*. 2013;**40**(11):111719.
  - [16] Chuter RW, Rixham PA, Weston SJ, Cosgrove VP. Feasibility of portal dosimetry for flattening filter-free radiotherapy. *J Appl Clin Med Phys*. 2016;**17**(1):112-20.
  - [17] Wendling M, Louwe RJ, McDermott LN, Sonke JJ, van Herk M, Mijnheer BJ. Accurate two-dimensional IMRT verification using a back-projection EPID dosimetry method. *Med Phys*. 2006;**33**(2):259-73.
  - [18] King BW, Greer PB. A method for removing arm backscatter from EPID images. *Med Phys*. 2013;**40**(7):071703.
  - [19] Chanton T, Thongsawad S, Saiyo N, Udee N. Evaluation of Dosimetric Characteristics of Electronic Portal Imaging Device (EPID) for Flattening Filter Free (FFF) Beams. *J Health Sci Med Res*. 2017;**35**(4):361-71.
  - [20] McNutt TR, Mackie TR, Reckwerdt P, Papanikolaou N, Paliwal BR. Calculation of portal dose using the convolution/superposition method. *Med Phys*. 1996;**23**(4):527-35.
  - [21] Boutry C, Sors A, Fontaine J, Delaby N, Delpon G. Technical Note: A simple algorithm to convert EPID gray values into absorbed dose to water without prior knowledge. *Med Phys*. 2017;**44**(12):6647-53.
  - [22] Zwan BJ, King BW, O'Connor DJ, Greer PB. Dose-to-water conversion for the backscatter-shielded EPID: a frame-based method to correct for EPID energy response to MLC transmitted radiation. *Med Phys*. 2014;**41**(8):081716.
  - [23] Boellaard R, Essers M, van Herk M, Mijnheer BJ. New method to obtain the midplane dose using portal in vivo dosimetry. *J Radiat Oncol Biol Phys*. 1998;**41**(2):465-74.
  - [24] Nelms BE, Rasmussen KH, Tome WA. Evaluation of a fast method of EPID-based dosimetry for intensity-modulated radiation therapy. *J Appl Clin Med Phys*. 2010;**11**(2):140-57.
  - [25] Bawazeer O, Herath S, Sarasanandarajah S, Kron T, Deb P. The Influence of Acquisition Mode on the Dosimetric Performance of an Amorphous Silicon Electronic Portal Imaging Device. *J Med Phys*. 2017;**42**(2):90-5.
  - [26] Yeo IJ, Jung JW, Patyal B, Mandapaka A, Yi BY, Kim JO. Conditions for reliable time-resolved dosimetry of electronic portal imaging devices for fixed-gantry IMRT and VMAT.

*Med Phys.* 2013;**40**(7):072102.

- [27] Low DA, Harms WB, Mutic S, Purdy JA. A technique for the quantitative evaluation of dose distributions. *Med Phys.* 1998;**25**(5):656–61.